Arsenic Concentration, Fraction, and Environmental Implication in Fe–Mn Nodules in the Karst Area of Guangxi

Wenbing Ji [1,2,3], Rongrong Ying [1,2,*], Zhongfang Yang [3,*], Zhewei Hu [1,2], Qiong Yang [4], Xu Liu [3], Tao Yu [5], Lei Wang [6], Jianxun Qin [6] and Tiansheng Wu [6]

1 Nanjing Institute of Environmental Sciences, Ministry of Ecology and Environment, Nanjing 210042, China
2 State Environmental Protection Key Laboratory of Soil Environmental Management and Pollution Control, Nanjing 210042, China
3 School of Earth Sciences and Resources, China University of Geosciences, Beijing 100083, China
4 School of Agricultural Sciences, Zhengzhou University, Zhengzhou 450001, China
5 School of Science, China University of Geosciences, Beijing 100083, China
6 Guangxi Institute of Geological Survey, Nanning 530023, China
* Correspondence: yrr@nies.org (R.Y.); yangzf@cugb.edu.cn (Z.Y.)

Abstract: We determined the concentrations, geochemical fractions, and potential environmental implications of arsenic (As) via pH-static extraction experiments, X-ray photoelectron spectroscopy (XPS), and sequential extraction. Compared with the corresponding soils, the enrichment factors followed the order As (4.27) > Fe (2.14) > P (1.71) > Mn (1.41) > Al (0.95) > Ti (0.44) > Si (0.39) > Mg (0.28) > K (0.13). As showed a higher enrichment factor than all other elements. Arsenic showed a high linear correlation with iron in the FMNs, which can be expressed as As = 18.68Fe − 175.89 ($r^2 = 0.97$, $p < 0.01$), indicating that Fe plays an important role in the geochemical behavior of As. Most of the As occurred as As (V) (83.79%) in the Fe–Mn nodules (FMNs), and As (III) (16.21%) only occupied a small portion. The distribution of As in the geochemical fractions of the FMNs followed the order F5 (99.54%) > F3 (0.25%) > F4 (0.10%) > F2 (0.09%) > F1 (0.02%), indicating that the residual fraction (F5) of As is the most dominant component. The total release of As from the nodules was extremely low (<0.01%) under neutral pH conditions (pH 6.0–8.0), and As was adsorbed and stabilized by the FMNs under neutral pH conditions (pH 6.0–8.0). However, overacidification or alkalization of the soil environment will promote As release, with subsequent ecological hazards.

Keywords: Fe–Mn nodule; arsenic; geochemical fraction; pH leaching experiment; environmental implication

1. Introduction

Arsenic (As), as an important metalloid element in the environment, has attracted considerable attention because of its valence, strong mobility, and toxic effects on organisms [1–3]. In the soil environment, As mainly occurs in its inorganic forms as As (III) and As (V), with a dynamic balance between them [4]. Arsenate (AsO_4^{3-}) and arsenite (AsO_3^{3-}) are the main species in soil environments [5,6]. The toxicity of As is closely related to its valence, and As (III) tends to be more toxic than As (V) [7]. Any changes in the state of As affect its mobility in soil [8]; under sufficient oxygen and drainage conditions, As (V) is the main form in soil and binds to iron oxides (hydroxides), making them stable and difficult to be desorbed [9]. As in soils is most commonly associated with its primary minerals derived from the parent material, secondary minerals (primarily Fe oxy/hydroxides; sulfides) formed in the course of mineral weathering, and As adsorbed to mineral surfaces [6,9]. As (V) will transform into the toxic and mobile form of As (III) with fluctuations in precipitation or groundwater level, increases in soil moisture, and decreases in the soil redox potential [10]. The chemical properties and stabilization mechanism of AsO_4^{3-} and AsO_3^{3-} are complex and differ from those of other heavy metals such as Pb

(II), Cd (II), Zn (II), Cu (II), and Ni (II). In this context, the stabilization of As and other heavy metal compounds in polluted soil is challenging. Although pH control agents, such as lime, fly ash, and phosphates, can be used for the stabilization of Pb, Zn, and Cd in soil, As is activated by higher pH levels [11,12]. Based on previous studies, iron salt can stabilize As in polluted soils, but the hydrolysis of Fe (II) and Fe (III) ions leads to soil acidification and increases the leaching concentrations of Pb (II), Cd (II), Zn (II), and other heavy metals [13,14].

Fe–Mn nodules (FMNs), which have universal distribution in most soil types, tend to accumulate various heavy metal elements and metalloids [15,16]. Although, generally, the total As concentration is applied in the evaluation of As contamination levels in FMNs, soils, and sediments, this does not provide sufficient information about its bioavailability or potential toxic effects [17–19]. The toxicity, migration, and biological availability of As are mainly determined by its chemical fractions in the FMNs [17,20]. Previous studies have focused on the geochemical behavior of heavy metals, such as Cr, Sb, Cd, Pb, Cu, Ni, and Zn, but they have largely ignored As in the FMNs. Moreover, so far, only a few studies have investigated the geochemical behavior of As and its environmental implications in FMNs under natural conditions, although studies on the chemical fractions of As in FMNs could provide a basis for assessing the contamination levels and toxicity risks and revealing the migration and enrichment characteristics of pollutants in soil. The karst areas are distribution areas with carbonate rocks as the main soil-forming parent material [16,21]. In 2015, the China Geological Survey released the Report on Geochemical Survey of Chinese Arable Land, and the survey results showed that 8.2% of heavy-metal-contaminated sites covered an area of 75,913 km^2, and the contaminated or over-standard arable land was mainly distributed in the southwest karst area, followed by the Southern China [21].

The city of Nanning is the capital of Guangxi Province, Southwest China, and located in the subtropical monsoon region with karst hydrology [16]. In this area, the concentrations of heavy metals are usually high because of secondary enrichment in the red soils and the wide distribution of FMNs in karst areas [16,21]. This study investigated the environmental implications of As in the FMNs of red soils in a typical karst area. We conducted pH-static extraction experiments, X-ray photoelectron spectroscopy (XPS), and sequential extraction to acquire sufficient information on the effects of FMNs on the geochemical behavior of As, with the aim to evaluate the environmental implications.

2. Materials and Methods

2.1. Study Area and Sampling Sites

Sampling was conducted in October 2018. Figure 1 shows a map of the study area. The main soil type is red soil derived from carbonate rocks with typical geological high background characteristics of As, and the area has a hot and humid tropical monsoon climate [16,21]. The topographic feature of the research area is dominant karst plains and low hills, and its main soil type is terra rossa derived from carbonate rocks. The nodules are relatively rich in the soils. It is a typical geological high background area [16].

2.2. Sample Pretreatment

Sixteen pieces of surface soil samples (0–20 cm) were collected in an extended area of 394 km^2 in Nanning of Guangxi in accordance with the Specification of Land Quality Geochemical Assessment (DZ/T 0295–2016) [16]. Each soil sample collected weighed approximately 2 kg; they were stored in polyethylene bags, air-dried for around 5 days, and sieved through 2-mm nylon sieves. During sieving, FMNs larger than 2 mm were manually collected, washed with deionized (DI) water (18.25 MΩ), and dried. They were mainly elliptical. The soil samples and the FMNs were ground to less than 200 meshes (<0.074 mm) for subsequent analysis.
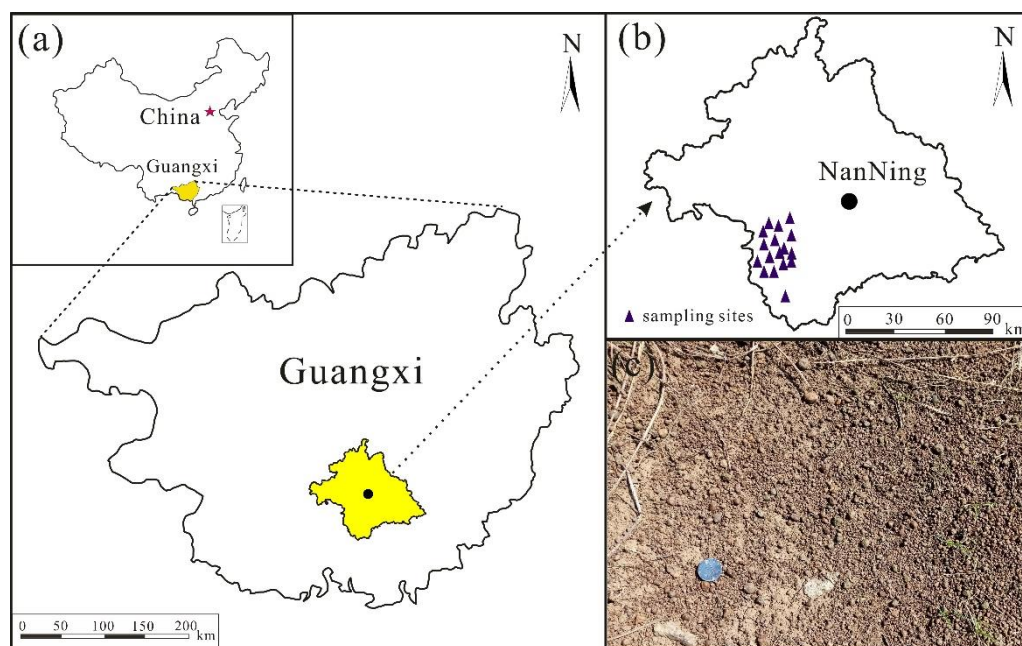
Figure 1. Map showing the study area in China (**a**), locations of the sampling sites (**b**), and image of the soil surface (**c**).

2.3. Chemical Analysis

2.3.1. The Elemental and MFN Concentrations

The total concentrations of Si, Ti, Al, Fe, Mn, Mg, Ca, Na, K, and P were determined through inductively coupled plasma atomic emission spectrometry (ICP-AES, Thermo Fisher Scientific, Waltham, MA, USA), and As was determined via atomic fluorescence spectrophotometry (AFS, Model AFS-230E; Kechuang Haiguang Instrument Co., Ltd., Beijing, China) after decomposition with HCl–HNO$_3$–HClO$_4$–HF [15]. Accuracy and precision were determined based on standard reference materials (GSS17, GSS22, GSS25, and GSS27) [19]. Calculation of the relative double difference (RD/%) is a method of controlling data quality, and the relative standard deviation was below 10% during the testing process.

2.3.2. pH-Dependent Leaching Experiments

To investigate the release of heavy metals as a function of pH, pH-dependent leaching experiments of FMNs were performed, as described elsewhere [15,16]. The potential release of selected trace elements (As, Cd, Cu, Mn, Pb, and Zn) from the sediments has been studied in the Cam River mouth (Vietnam) under the influence of pH, using the same method [22]. The leaching experiments were conducted at 20 °C for 48 h. Briefly, Fe–Mn nodule powder (1 g) was placed in a centrifuge polypropylene tube (50 mL), and 9.6 mL of DI water was added to obtain a final ratio of approximately 10. Ten pH values (2, 3, 4, 5, 6, 7, 8, 9, 10, and 11) were selected to represent the pH changes in the soil environment, using NaOH (2 M or 1 M) and HNO$_3$ (1 M or 0.1 M) for adjustment. The reactors were stirred for 48 h, and the filtrated leachate was measured through ICP–MS (Thermo Electron Co X-SERIES, Waltham, MA, USA) and AFS (Model AFS-230E; Kechuang Haiguang Instrument Co., Ltd., Shanghai, China). Accuracy and precision were determined based on standard reference materials (GSS17, GSS22, GSS25, and GSS27) [19]. The relative standard deviation was below 10%.

2.3.3. Sequential Extraction

The FMNs with a gradient of As were selected in the modified sequential extraction, as described elsewhere [23]. This methodology allowed the separation of As into five chemical fractions, namely (1) F1, nonspecifically adsorbed phase (using 0.05 M (NH$_4$)$_2$SO$_4$, solid/solution = 25:1, shaking for 4 h at 20 °C); (2) F2, specifically adsorbed

phase (using 0.05 M $NH_4H_2PO_4$, solid/solution = 25:1, shaking for 16 h at 20 °C); (3) F3, amorphous hydrous oxides/oxyhydroxides of Fe (Mn, Al) (using 0.2 M NH_4-oxalate at pH = 3.25, solid/solution = 25:1, shaking for 4 h at 20 °C); (4) F4 crystalline hydrous oxides/oxyhydroxides of Fe (Mn, Al), (using 0.2 M NH_4-oxalate + 0.1 M ascorbic acid at pH = 3.25, solid/solution = 25:1, shaking for 30 min at 96 °C); and (5) F5, residual phases (using HF–HNO$_3$–HClO$_4$, shaking for 72 h at 65 °C). The filtrated leachate was measured through ICP–MS (Thermo Electron Co X-SERIES, America) and AFS (Model AFS-230E; Kechuang Haiguang Instrument Co., Ltd., China); accuracy and precision were calculated by comparing the sum of the concentrations of the F1–F5 fractions with the total concentrations, and the average FMN recoveries were $89.57 \pm 3.12\%$, indicating that the test data quality of sequential extraction was reliable.

2.3.4. XPS Analysis

The FMN powders were measured using an ESCALLAB MKIII photoelectron spectrometer with an MgKα X-ray source through X-ray photoelectron spectroscopy (XPS) analysis [24]. The instrument was operated at a pressure of 3×10^{-8} Pa and θ = 40°; energy accuracy was ±0.1 eV. The XPS survey and narrow scan spectra of As2p3/2 with high precision were recorded, and the quality and chemical states of As were measured on the basis of the decomposed and curve fitting spectra (Ordinary Least Squares). The binding energy of C1s (EB = 284.60 eV) was used to correct the other recorded binding energies. XPS is a surface analysis technique to study the composition and ionic state of the surface layer of a substance of FMNs. We used Avantage Surface Chemical Analysis Software to analyze the results. By comparing the energy of the electrons in different shell layers of the atoms or ions of known elements, the composition and state of the atoms or ions in the surface layer of the unknown sample can be determined.

2.4. Statistical Analysis

We used IBM SPSS ver. 22 to calculate and process Pearson's correlation coefficients. The graphs were generated using ArcGIS 10.6 and retouched with CorelDRAW X7.
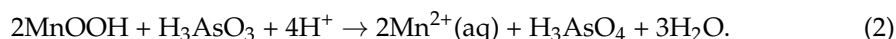
3. Results and Discussion

3.1. Concentrations of FMNs in Soils

Table 1 shows the concentrations of FMNs in the corresponding soils. The enrichment factors followed the order As (4.27) > Fe (2.14) > P (1.71) > Mn (1.41) > Al (0.95) > Ti (0.44) > Si (0.39) > Mg (0.28) > K (0.13). The enrichment coefficients of different elements in FMNs are closely related to the geochemical behavior. Whilst As, Fe, P, and Mn showed different degrees of enrichment, Al, Ti, Si, Mg, and K showed varying degrees of loss in the FMNs; this was particularly the case for alkaline ions, which tend to easily dissolve and migrate with water. The relatively insoluble substances (Fe, Mn) and other heavy metals tend to remain in situ [16,21]. The concentrations of manganese varied largely, whereas those of iron remained in a stable range in the FMNs (Table 1). This difference is mainly related to the surrounding soil matrices [25]. The main components of the FMNs were Al, Si, Fe, and Mn, which is consistent with the composition of the average upper continental crust [26]. In previous studies, the average concentrations of FMNs in the main soil types of China followed the order Si > Fe > Al > Mn > Mg > Ca > Ti > K > Na > P [27]. Both Fe and Mn are variable valence elements, which is of great importance for the formation of nodules [15,28,29]. Based on previous studies, Al and Si contained in the FMNs are enriched in clay minerals and quartz, respectively [25,30]. Arsenic showed a high linear correlation with iron in the FMNs, which can be expressed as As = 18.68Fe − 175.89 (r^2 = 0.97, $p < 0.01$), indicating that Fe plays an important role in the geochemical behavior of As. Table 2 shows the matrix correlation coefficients among the element content in the FMNs; As strongly correlated with iron and phosphorus ($r_{As–Fe}$ = 0.985, $r_{As–P}$ = 0.670, $p < 0.01$). Together with phosphorus (P), arsenic belongs to the fifth main group of the periodic table. Arsenic shares

chemical similarity with phosphorus. Both of them can be adsorbed on the surfaces of Fe–Mn nodules. Therefore, As is also correlated with phosphorus [23].

In a previous study in the Morvan Region in France, the distribution map of FMNs was determined through X-ray synchrotron microfluorescence analysis, showing that As is highly correlated with Fe, and the As/Fe ratio was stable throughout the entire nodule [31]. The Mn/Fe oxides, especially Mn oxides, such as oxidize arsenic [As(III)] to As(V), which are less soluble, play an important role in the valence change in As [31]. The oxidation of As by Mn can be divided into two steps [32]:

$$2MnO_2 + H_3AsO_3 + H_2O \rightarrow 2MnOOH + H_3AsO_4, \tag{1}$$

$$2MnOOH + H_3AsO_3 + 4H^+ \rightarrow 2Mn^{2+}(aq) + H_3AsO_4 + 3H_2O. \tag{2}$$

3.2. Geochemical Fractions of As in FMNs

Table 3 shows the geochemical fractions of As in the FMNs, determined through sequential extraction. The nonspecifically adsorbed fraction, which is the most mobile fraction, was extremely low (mean at 0.02%). The specifically adsorbed fraction was 0.09% because of the adsorption phenomenon caused by the specific force between the colloidal surface and As. The nonspecifically (F1) and specifically (F2) adsorbed fractions of As are potentially hazardous to watersheds because they are the most mobile As fractions in the soil systems, with considerable toxicity [18,19]. The amorphous hydrous oxides/oxyhydroxides of Fe (Mn, Al) (F3) and crystalline hydrous oxides/oxyhydroxides of Fe (Mn, Al) (F4) phases of As were 0.25% and 0.10%, respectively. As is preferentially adsorbed on Fe (Mn, Al) oxides/oxyhydroxides via sorption and/or co-precipitated to control its attenuation and mobility. The resulting effect probably caused the release of additional As into the water [19,20]. The geochemical fractions of As show increased stability from F1 to F5, and the residual fraction is considered to be in a stable state because of the robust limitation of its mineral crystal structure [18]. The residual fraction of As means As$_{total}$—the sum of fractions F1–F4—which represents the arsenic that enters the interior of the mineral lattice, which is very stable and generally cannot be extracted. In this study, the residual phase accounted for 99.54%, indicating that As was extremely stable in the FMNs. The residual phase in this study was more pronounced compared to previous findings on As in sediments or soils [6,35]. However, in surface sediments from the Dan River drainage basin, the residual fraction was the major phase [36].

3.3. Bioavailability of As in FMNs and Its Environmental Implications

The XPS results of As and the high-resolution XPS spectrum of As3d are shown in Table 4 and Figure 2, respectively. Most of the As occurred as As (V) (83.79%), and As (III) (16.21%) only accounted for a small portion, mainly related to the formation of nodules. In a previous study, Mn had a high valence state, and Mn (III) and Mn (IV) accounted for 42.72% and 57.28% of the total manganese, respectively; this indicates that the variable elements tend to be in a high valence state in FMNs, and FMNs may not be formed under fully oxidized conditions [24].

Table 1. Concentrations of elements in FMNs and the corresponding soils.

Samples	Fe	Mn	Al	Si	Mg	K	P	Ti	As	Reference
	%	%	%	%	%	%	%	%	%	
FMNs (*n* = 16)	19.52 ± 2.61 (13.82–22.50)	2.33 ± 3.52 (0.35–13.50)	13.09 ± 2.41 (8.70–16.58)	7.66 ± 2.40 (5.77–12.78)	0.07 ± 0.03 (0.04–0.14)	0.040 ± 0.04 (0.02–0.14)	2.10 ± 0.53 (1.37–3.30)	7.31 ± 1.07 (5.52–10.43)	0.19 ± 0.049 (0.081–0.232)	This study
Corresponding soils (*n* = 16)	9.13 ± 2.40 (6.08–12.41)	1.65 ± 1.36 (0.01–4.98)	13.74 ± 2.98 (8.52–16.68)	19.66 ± 2.55 (16.54–25.24)	0.25 ± 0.16 (0.08–0.73)	0.31 ± 0.35 (0.108–1.544)	1.23 ± 0.68 (0.43–2.32)	16.49 ± 7.11 (9.65–29.85)	0.044 ± 0.01 (0.028–0.061)	This study
Lateritic subsoil	12.82	7.05	14.81	14.93	0.12	0.14	0.61	20.71	0.29	[33]
FMNs	29.24	10.07	6.64	6.86	0.13	0.27	1.40	8.88	1.25	[33]
FMNs	8.11	6.41	2.84	29.6	0.236	0.449	/	/	0.023	[15]
Average upper crustal composition (AUCC)	3.91	0.77	8.15	31.14	1.50	2.32	0.65	5.12	0.005	[26]
Background soil (Guangxi)	2.90	0.30	7.09	33.86	0.28	0.95	/	/	0.015	[34]
Background soil (China)	3.28	0.60	6.67	30.39	1.09	2.08	0.52	4.30	0.010	[21]
Enrichment factor *	2.14	1.41	0.95	0.39	0.28	0.13	1.71	0.44	4.27	/

Notes: * Enrichment factor, calculated as the ratio of element concentration in the nodules to that in the corresponding soil [25]. Results are presented as mean values ± standard error, and values in parentheses show the ranges for each element in the samples. Literature data are provided as mean concentrations.

Table 2. Correlation matrix showing the coefficients for the different elements in the FMNs (*n* = 16).

	Fe	Mn	Si	Al	Mg	Ca	Na	K	P	Ti	As
Fe	1										
Mn	0.284	1									
Si	−0.783 **	0.209	1								
Al	−0.806 **	−0.653 **	0.284	1							
Mg	0.478	0.774 **	0.148	−0.853 **	1						
Ca	−0.319	0.474	0.576 *	−0.002	0.447	1					
Na	0.409	0.802 **	0.167	−0.767 **	0.964 **	0.573 *	1				
K	0.371	0.719 **	0.244	−0.801 **	0.956 **	0.374	0.908 **	1			
P	0.749 **	0.509 *	−0.229	−0.914 **	0.892 **	0.146	0.812 **	0.845 **	1		
Ti	0.164	0.032	0.076	−0.355	0.380	−0.175	0.334	0.586 *	0.456	1	
As	0.985 **	0.265	−0.832 **	−0.746 **	0.392	−0.378	0.333	0.295	0.670 **	0.137	1

Notes: *, ** significant at $p < 0.05$ and 0.01, respectively; FMNs = Fe–Mn nodules.

Table 3. Distribution of arsenic in geochemical fractions of the FMNs.

Samples	F1	F2	F3	F4	F5	References
	%	%	%	%	%	
Fe–Mn nodules (*n* = 5)	0.02 ± 0.01 (0.01–0.04)	0.09 ± 0.05 (0.04–0.16)	0.25 ± 0.29 (0.04–0.61)	0.10 ± 0.07 (0.03–0.19)	99.54 ± 0.42 (99.00–99.86)	This study
Sediments (*n* = 18)	0.18	15.91	30.27	12.38	41.25	[19]

Notes: FMNs = ferromanganese nodules; F1 = nonspecifically adsorbed fraction; F2 = specifically adsorbed fraction; F3 = amorphous hydrous oxides/oxyhydroxides of Fe (Mn, Al) fraction; F4 = crystalline hydrous oxides/oxyhydroxides of Fe (Mn, Al) fraction; F5 = residual fraction. Results are presented as mean values ± standard error, and values in parentheses show the ranges for each metal in the samples. Literature data are given as mean concentrations.
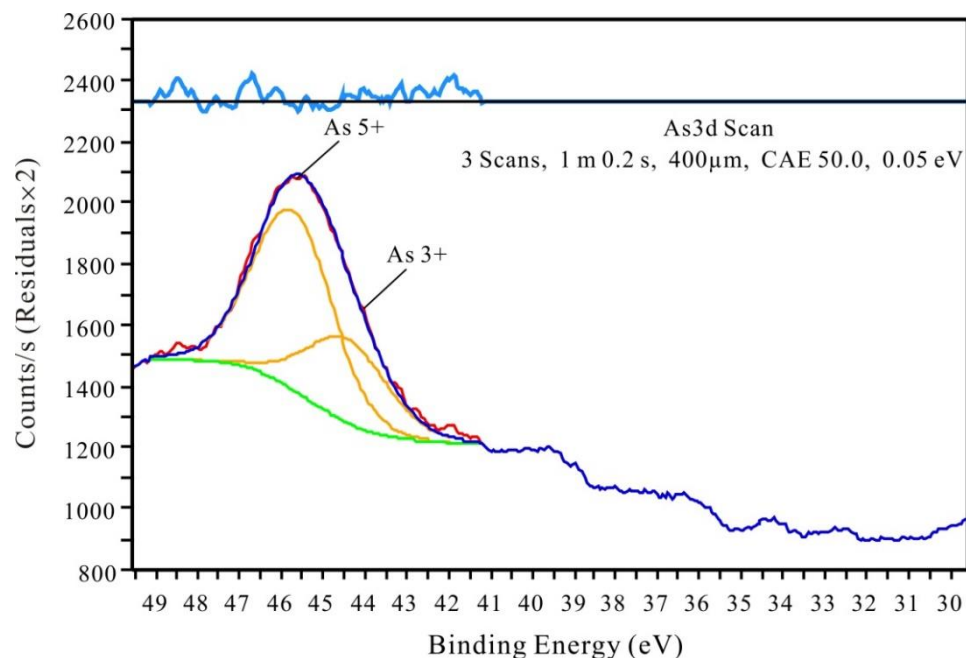

Figure 2. High-resolution XPS spectrum of As3d in the ferromanganese nodule powder.

Table 4. As$_{2p}$3/2 electron binding energy and atomic percentages.

Name	Start BE	Peak BE	End BE	Height CPS	FWHM eV	Atomic (%)
As (V)	49.15	45.67	41.25	762.43	2.60	83.79
As (III)	49.15	44.03	41.25	248.95	1.54	16.21

Notes: BE = binding energy; CPS = count per second; FWHM = full width at half maxima.

Table 4 shows the dissolution results of As, Al, Fe, and Mn from the FMNs in pH-static leaching experiments. Under acidic conditions, As, Al, Fe, and Mn showed high solubility; at pH 2, 0.44% of the total As amount was released. The dissolution of As gradually decreased when the pH value increased from 2 to 7, whereas it gradually increased at a pH from 7 to 11, indicating that As is an amphoteric element. Both Mn and Fe oxides can sorb trace elements. The adsorption of cationic elements increases with increasing pH, whereas that of arsenic (As [V]) shows the opposite trend [20]. Although Al has a relatively high solubility (≥0.09%) at a pH from 2 to 3, its solubility was low (<0.01%) when the pH value ranged from 3 to 11 (Table 5). Under alkaline conditions (pH ≥ 7), Al showed no dissolution. The dissolution of Mn gradually decreased when the pH increased from 2 to 11. The pH leaching experiment demonstrates that the total release of As from the nodules is extremely low under weakly acidic conditions (pH 6.0–7.0, <0.01%) (Table 5). Compared with other heavy metals, such as Cd, Pb, Zn, Ni, and Cu, As shows a certain dissolution under alkaline conditions [16]. The desorption performance of arsenic tends to be large when the soil pH is high, resulting in the low adsorption of arsenic on the surfaces of minerals. Based on a previous study, the higher the dissolution of arsenic, the greater the content of arsenic in the soil solution [37], mainly because the number of positively charged ions on the soil colloid surface decreases with an increasing pH value, and the participation of OH^- or H^+ in the adsorption and desorption causes the dissociation of soil colloids and arsenic ions, thereby affecting the adsorption of arsenic and leading to the increase in water-soluble arsenic in soil [20,37]. Both As and Al displayed a V-shaped pH-dependent leaching pattern, with significant releases at a pH range from 2 to 11. The addition of phosphate considerably increased the amount of As released into the solution throughout the entire pH range studied and changed the desorption edge profile in the estuarine sediment, which exhibited a V-shaped profile, with the increase in As release at acidic and alkaline pH values [38]. In a previous study, heavy metals (Cd, Cu, Mn, Pb, and Zn) and arsenic in the sediments displayed a V-shaped pH-dependent leaching pattern, with important releases at a pH range from 2 to 11 [22].

Table 5. Dissolution of As, Al, Fe, and Mn from FMNs in pH-static leaching experiments.

pH	As		Al		Fe		Mn	
	mg/kg	Dissolution (%)	mg/kg	Dissolution (%)	mg/kg	Dissolution (%)	mg/kg	Dissolution (%)
2	0.93	0.44	890.02	0.70	330.0	0.16	7.36	1.03
3	0.76	0.36	120.16	0.09	14.40	0.01	5.19	0.73
4	0.07	0.04	1.24	<0.01	3.44	<0.01	1.77	0.25
5	0.07	0.03	1.20	<0.01	3.54	<0.01	1.22	0.17
6	0.03	<0.01	0.38	<0.01	1.35	<0.01	1.07	0.15
7	nd *	nd	0.47	<0.01	1.80	<0.01	0.98	0.14
8	nd	nd	0.37	<0.01	3.43	<0.01	0.91	0.13
9	0.06	0.03	0.32	<0.01	3.38	<0.01	0.82	0.11
10	0.06	0.03	0.31	<0.01	2.43	<0.01	0.55	0.08
11	0.07	0.04	1.20	<0.01	2.34	<0.01	0.05	0.01

Notes: FMNs = Fe–Mn nodules; nd * = not determined.

4. Conclusions

Overall, compared with the corresponding soils, the enrichment factors followed the order As (4.27) > Fe (2.14) > P (1.71) > Mn (1.41) > Al (0.95) > Ti (0.44) > Si (0.39) > Mg (0.28) > K (0.13). Whilst As, Fe, P, and Mn showed different degrees of enrichment, Al, Ti, Si, Mg, and K showed varying degrees of loss. Arsenic showed a good linear correlation with iron in the FMNs and most occurred in the form of As (V) (83.79%), whereas As (III) (16.21%) only occupied a small portion. The distribution of As in the geochemical fractions of the FMNs followed the order F5 (99.54%) > F3 (0.25%) > F4 (0.10%) > F2 (0.09%) > F1 (0.02%), indicating that the residual fraction (F5) of As was the most dominant component. The total released amount of As from the nodules was extremely low (<0.01%) under

neutral conditions (pH 6.0–8.0), whereas, under strong acidity and alkalinity, As dissolution increased. Under neutral conditions, As tends to be adsorbed and stabilized by FMNs, indicating that it has a low impact on the soil environment. However, overacidification or alkalization of the soil environment can promote the release of As, resulting in subsequent ecological hazards.

References

1. Gibert, O.; Pablo, J.; Cortina, J.; Ayora, C. In situ removal of arsenic from groundwater by using permeable reactive barriers of organic matter/limestone/zero-valent iron mixtures. *Environ. Geochem. Health* **2010**, *32*, 373–378. [CrossRef]
2. Wu, C.; Cui, M.Q.; Xue, S.G.; Li, W.C.; Huang, L.; Jiang, X.X.; Qian, Z.Y. Remediation of arsenic-contaminated paddy soil by iron-modified biochar. *Environ. Sci. Pollut. Res.* **2018**, *25*, 20792–20801. [CrossRef]
3. Chanpiwat, P.; Hensawang, S.; Suwatvitayakorn, P.; Ponsin, M. Risk assessment of bioaccessible arsenic and cadmium exposure through rice consumption in local residents of the Mae Tao Sub-district, Northwestern Thailand. *Environ. Geochem. Health* **2019**, *41*, 343–356. [CrossRef]
4. Antman, K.H. Introduction: The history of arsenic trioxide in cancer therapy. *Oncologist* **2001**, *6*, 1–2. [CrossRef]
5. Gasparatos, D. Sequestration of heavy metals from soil with Fe–Mn concretions and nodules. *Environ. Chem. Lett.* **2013**, *11*, 1–9. [CrossRef]
6. Duan, Y.H.; Gan, Y.Q.; Wang, Y.X.; Liu, C.X.; Yu, K.; Deng, Y.M.; Zhao, K.; Dong, C.J. Arsenic speciation in aquifer sediment under varying groundwater regime and redox conditions at Jianghan Plain of Central China. *Sci. Total Environ.* **2017**, *607–608*, 992–1000. [CrossRef] [PubMed]
7. Qi, P.F.; Pichler, T. Competitive adsorption of As(III), As(V), Sb(III) and Sb(V) onto ferrihydrite in multi-component systems: Implications for mobility and distribution. *J. Hazard. Mater.* **2017**, *330*, 142–148. [CrossRef]
8. Gasparatos, D.; Haidouti, C.; Tarenidis, D. Characterization of iron oxides in Fe–rich concretions from an imperfectly drained Greek soil: A study by selective–dissolution techniques and X–ray diffraction. *Arch. Agron. Soil Sci.* **2005**, *50*, 485–493. [CrossRef]
9. Bose, P.; Sharma, A. Role of iron in controlling speciation and mobilization of arsenic in subsurface environment. *Water Res.* **2002**, *36*, 4916–4926. [CrossRef]
10. Smith, E.; Naidu, R.; Alston, A.M. Arsenic in the Soil Environment: A Review. *Adv. Agron.* **1998**, *64*, 149–195.
11. Kumpiene, J.; Lagerkvist, A.; Maurice, C. Stabilization of As, Cr, Cu, Pb and Zn in soil using amendments—A review. *Waste Manag.* **2008**, *28*, 215–225. [CrossRef]
12. Miretzky, P.; Cirelli, A.F. Remediation of Arsenic-Contaminated Soils by Iron Amendments: A Review. *Crit. Rev. Environ. Ence Technol.* **2010**, *40*, 93–115. [CrossRef]
13. Kim, J.Y.; Davis, A.P.; Kim, K.W. Stabilization of Available Arsenic in Highly Contaminated Mine Tailings Using Iron. *Environ. Sci. Technol.* **2003**, *37*, 189–195. [CrossRef]
14. Moore, T.J.; Rightmire, C.M.; Vempati, R.K. Ferrous iron treatment of soils contaminated with arsenic-containing wood-preserving solution. *Soil Sediment Contam.* **2000**, *9*, 375–405. [CrossRef]
15. Ettler, V.; Chren, M.; Mihaljevič, M.; Drahota, P.; Křížek, B.; Veselovský, F.; Sracek, O.; Vaněk, A.; Penížek, V.; Komárek, M.; et al. Characterization of Fe–Mn concentric nodules from luvisol irrigated by mine water in a semi–arid agricultural area. *Geoderma* **2017**, *299*, 32–42. [CrossRef]
16. Ji, W.B.; Yang, Z.F.; Yu, T.; Yang, Q.; Wen, Y.B.; Wu, T.S. Potential ecological risk assessment of heavy metals in the Fe–Mn nodules in the karst area of Guangxi, Southwestern China. *Bull. Environ. Contam. Toxicol.* **2021**, *106*, 51–56. [CrossRef]
17. Sundaray, S.K.; Nayak, B.B.; Lin, S.; Bhatta, D. Geochemical speciation and risk assessment of heavy metals in the river estuarine sediments-a case study: Mahanadi basin, India. *J. Hazard. Mater.* **2011**, *186*, 1837–1846. [CrossRef]

18. Wang, H.T.; Liu, R.M.; Wang, Q.R.; Xu, F.; Men, C.; Shen, Z. Bioavailability and risk assessment of arsenic in surface sediments of the Yangtze River estuary. *Mar. Pollut. Bull.* **2016**, *113*, 125–131. [CrossRef]

19. Wang, H.B.; Xu, J.M.; Mario, A.G.; Shi, Z.L.; Li, S.F.; Zang, S.Y. Arsenic concentration, speciation, and risk assessment in sediments of the Xijiang River basin, China. *Environ. Monit. Assess* **2019**, *191*, 663–674. [CrossRef]

20. Suda, A.; Makino, T. Functional effects of manganese and iron oxides on the dynamics of trace elements in soils with a special focus on arsenic and cadmium: A review. *Geoderma* **2016**, *270*, 68–75. [CrossRef]

21. Wen, Y.B.; Li, W.; Yang, Z.F.; Zhang, Q.Z.; Ji, J.F. Enrichment and source identification of Cd and other heavy metals in soils with high geochemical background in the karst region, Southwestern China. *Chemosphere* **2020**, *245*, 125620. [CrossRef]

22. Huu, H.H.; Rudy, S.; Valérie, C.; Elvira, V.; Tom, V.G.; Tan, V.T. Potential release of selected trace elements (As, Cd, Cu, Mn, Pb and Zn) from sediments in cam river-mouth (Vietnam) under influence of pH and oxidation. *Sci. Total Environ.* **2012**, *435–436*, 487–498.

23. Wenzel, W.W.; Kirchbaumer, N.; Prohaska, T.; Domy, C.A.; Lombic, E.; Adrianod, D.C. Arsenic speciation in soils using an improved sequential extraction procedure. *Anal. Chim. Acta* **2001**, *436*, 309–323. [CrossRef]

24. Tan, W.F.; Liu, F.; Feng, X.H.; Huang, Q.Y.; Li, X.Y. Adsorption and redox reactions of heavy metals on Fe–Mn nodules from chinese soils. *J. Colloid Interface Sci.* **2005**, *284*, 600–605. [CrossRef]

25. Palumbo, B.; Bellanca, A.; Neri, R.; Roe, M.J. Trace metal partitioning in Fe–Mn nodules from Sicilian soils, Italy. *Chem. Geol.* **2001**, *173*, 257–269. [CrossRef]

26. Rudnick, R.L.; Gao, R. Composition of the continental crust. In *The Crust. Treatise on Geochemistry*; Rudnick, R.L., Ed.; Elsevier: Amsterdam, The Netherlands, 2003; pp. 1–64.

27. Tan, W.F.; Liu, F.; Li, Y.H.; Hu, H.Q.; Huang, Q.Y. Elemental composition and geochemical characteristics of iron–manganese nodules in main soils of China. *Pedosphere* **2006**, *16*, 72–81. [CrossRef]

28. Szymański, W.; Skiba, M.; Błachowski, A. Mineralogy of Fe–Mn nodules in Albeluvisols in the Carpathian Foothills. *Poland. Geoderma* **2014**, *218*, 102–110. [CrossRef]

29. Yu, X.L.; Lu, S.G. Micrometer-scale internal structure and element distribution of Fe-Mn nodules in Quaternary red earth of Eastern China. *J. Soils Sediments* **2016**, *16*, 621–633. [CrossRef]

30. Ettler, V.; Tomášová, Z.; Komárek, M.; Mihaljevič, M.; Šebek, O.; Michálková, Z. The pH dependent long–term stability of amorphous manganese oxide in smelter–polluted soils: Implication for chemical stabilization of metals and metalloids. *J. Hazard. Mater.* **2015**, *286*, 386–394. [CrossRef]

31. Manceau, A.; Tamura, N.; Celestre, R.S.; Alastair, A.M.; Nicolas, G.; Garrison, S.; Howard, A.P. Molecular-scale speciation of Zn and Ni in soil ferromanganese nodules from loess soils of the Mississippi basin. *Environ. Sci. Technol.* **2003**, *37*, 75–80. [CrossRef]

32. Nesbitt, H.; Canning, G.; Bancroft, G. XPS study of reductive dissolution of 7 Å-birnessite by H_3AsO_3, with constraints on reaction mechanism. *Geochim. Cosmochim. Acta* **1998**, *62*, 2097–2110. [CrossRef]

33. Neaman, A.; Mouélé, F.; Trolard, F.; Bourrié, G. Improved methods for selective dissolution of Mn oxides: Applications for studying trace element associations. *Appl. Geochem.* **2004**, *19*, 973–979. [CrossRef]

34. Zheng, G.D. Factors Influencing the Distribution and Accumulation of Heavy Metals in Topsoil Across Beibu Gulf of Guangxi. Master's Dissertation, China University of Geosciences, Beijing, China, 2016; pp. 17–18.

35. Baumann, Z.; Fisher, N.S. Relating the sediment phase speciation of arsenic, cadmium, and chromium with their bioavailability for the deposit-feeding polychaete nereis succinea. *Environ. Toxicol. Chem.* **2011**, *30*, 747–756. [CrossRef]

36. Meng, Q.; Zhang, J.; Feng, J.; Zhang, Z.; Wu, T. Geochemical speciation and risk assessment of metals in the river sediments from dan river drainage, China. *Chem. Ecol.* **2016**, *32*, 221–237. [CrossRef]

37. Cullen, W.R.; Reimer, K.J. Arsenic speciation in the environment. *Chem. Rev.* **1989**, *89*, 713–716. [CrossRef]

38. Rubinos, D.A.; Iglesias, L.; Francisco, D.F.; María, T.B. Interacting effect of ph, phosphate and time on the release of arsenic from polluted river sediments (anllóns river, spain). *Aquat. Geochem.* **2011**, *17*, 281–306. [CrossRef]